Geochemistry Geophysics Geosystems G3
AN ELECTRONIC JOURNAL OF THE EARTH SCIENCES
Published by AGU and the Geochemical Society

Article
Volume 7, Number 10
31 October 2006
Q10015, doi:10.1029/2006GC001251
ISSN: 1525-2027

Alkenone temperature anomalies in the Brazil-Malvinas Confluence area caused by lateral advection of suspended particulate material

Carsten Rühlemann
Bundesanstalt für Geowissenschaften und Rohstoffe, Referat Meeresgeologie und Tiefseebergbau, Stilleweg 2, D-30655 Hannover, Germany (c.ruehlemann@bgr.de)

Martin Butzin
Zentrum für Marine Umweltwissenschaften, Universität Bremen, Leobener Strasse, D-28359 Bremen, Germany

[1] Alkenone temperatures derived from suspended particulate organic material which was collected in austral summer 2001 from surface waters (5 m) south of the Brazil-Malvinas Confluence deviate from measured temperatures by −4° to −7°C when $U^{K'}_{37}$ ratios are converted to temperature using the Müller et al. (1998) calibration and up to −3°C when using the calibration of Conte et al. (2006). In contrast, alkenone temperatures determined from particulate material sampled north of the confluence reveal close correspondence to in situ temperatures or show slightly higher values. We suggest that the southern samples are biased by suspended organic detritus originating from the cold subpolar waters of the northward flowing Malvinas Current, whereas the northern samples carry an $U^{K'}_{37}$ signal of tropical/subtropical origin, transported southward with the Brazil Current. On the basis of surface ocean transport pathways and velocities simulated with the large-scale geostrophic (LSG) ocean general circulation model, we identify areas of the world ocean where alkenone temperatures are potentially biased to higher or lower values due to long particle residence times and lateral advection by surface currents.

Components: 8941 words, 8 figures, 1 table.

Keywords: alkenones; particle transport; Brazil-Malvinas Confluence; paleotemperature proxy.

Index Terms: 4558 Oceanography: Physical: Sediment transport (1862); 4850 Oceanography: Biological and Chemical: Marine organic chemistry (0470, 1050); 4255 Oceanography: General: Numerical modeling (0545, 0560).

Received 18 January 2006; **Revised** 29 June 2006; **Accepted** 7 August 2006; **Published** 31 October 2006.

Rühlemann, C., and M. Butzin (2006), Alkenone temperature anomalies in the Brazil-Malvinas Confluence area caused by lateral advection of suspended particulate material, *Geochem. Geophys. Geosyst.*, *7*, Q10015, doi:10.1029/2006GC001251.

1. Introduction

[2] Over the past decade, the alkenone method for reconstructing sea surface temperatures (SST) has become a major tool in paleoclimate research. Alkenones are synthesized by a limited number of planktic marine microalgae of the class *Prymnesiophyceae*, most notably the cosmopolitan coccolithophore *Emiliania huxleyi* and the closely related species *Gephyrocapsa oceanica* [*Jordan and Kleijne*, 1994; *Young and Bown*, 1997]. *E. huxleyi* is considered to be the major producer today and is the most widespread coccolithophore living in the modern ocean. Its distribution ranges

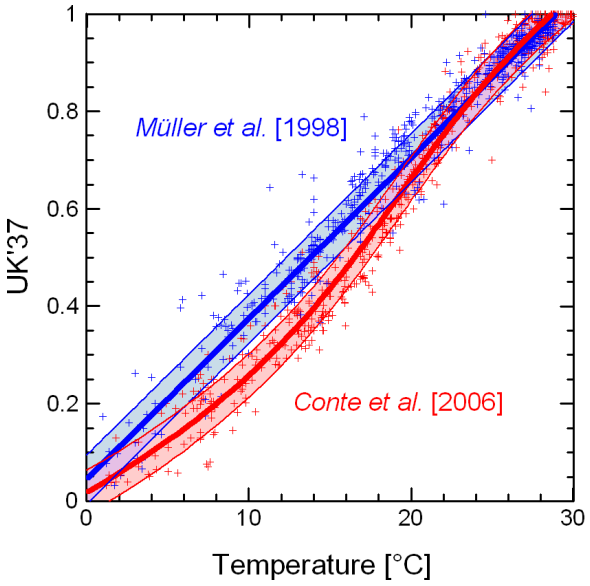

Figure 1. Comparison between the global $U^{K'}_{37}$ temperature calibrations of *Müller et al.* [1998] based on core top sediments and the calibrations of *Conte et al.* [2006] based on suspended particulates sampled from the mixed layer (usually from the upper 10 m of the water column). Core top sediment $U^{K'}_{37}$ data are plotted against overlying annual mean sea surface temperatures at 0 m water depth, as obtained from the *World Ocean Atlas 2001* [*Conkright et al.*, 2002]. Surface water $U^{K'}_{37}$ data are plotted against measured water temperatures at sampling depth. The calibration lines are shown with their mean standard errors of estimation.

from the nutrient-rich polar region to the oligotrophic tropical ocean, with relative abundances often reaching 60–80% [*Winter et al.*, 1994]. Coccolithophores synthesize long-chain (C_{37}–C_{39}), unsaturated ketones (alkenones) whose extent of unsaturation (number of double bonds) depends on the growth temperatures of the algae [*Brassell et al.*, 1986; *Prahl and Wakeham*, 1987].

[3] Core top measurements carried out on sediments collected between 60°N and 60°S in the world ocean reveal a linear correlation between the $U^{K'}_{37}$ index ($U^{K'}_{37} = [C_{37:2}]/([C_{37:2}] + [C_{37:3}])$ [*Prahl and Wakeham*, 1987]) and atlas values of mean annual surface water temperature [*Müller et al.*, 1998]. A recent compilation of global surface ocean C_{37} alkenone unsaturation data resulted in a nonlinear calibration [*Conte et al.*, 2006] where surface water $U^{K'}_{37}$ is consistently lower than core top $U^{K'}_{37}$ for temperatures <22°C (Figure 1). Other factors potentially influencing the $U^{K'}_{37}$ signal such as salinity [*Sikes and Sicre*, 2002], growth rate [*Popp et al.*, 1998], or differential degradation of diunsaturate and triunsaturated alkenones [*Prahl et al.*, 2003] appear to have a comparatively minor effect on the signal. Therefore $U^{K'}_{37}$, when measured in marine sediments can be converted into reliable estimates of sea surface temperature throughout most of the world ocean. Recent studies have suggested, however, that horizontal advection of particulate organic material (POM) in surface and deep waters may limit the interpretation of alkenone-based SST estimates in certain ocean areas [*Thomsen et al.*, 1998; *Benthien and Müller*, 2000; *Hamanaka et al.*, 2000; *Ohkouchi et al.*, 2002; *Sachs and Anderson*, 2003; *Müller and Fischer*, 2004; *Sicre et al.*, 2005].

[4] *Thomsen et al.* [1998] attributed strong deviations between measured water temperatures and $U^{K'}_{37}$ temperatures determined from sediment trap samples from the Norwegian Sea and Barents Sea to resuspension and lateral advection of organic detritus. *Benthien and Müller* [2000] observed that core top sediments recovered from the Brazil-Malvinas Confluence (BMC) area (35°–39°S) and the Argentine continental slope between 41° and 48°S generally yield 3 to 6 °C lower alkenone temperatures relative to annual mean modern SSTs. As the most likely cause for the anomalously low $U^{K'}_{37}$ values, *Benthien and Müller* [2000] suggested lateral displacement of suspended particles and sediments by strong northward surface and bottom currents, benthic storms, and downslope processes. *Hamanaka et al.* [2000] ascribed the difference between $U^{K'}_{37}$ from suspended particles and $U^{K'}_{37}$ from newly produced alkenones in the Sagami Bay (Japan) to the contribution of laterally transported detritus from alkenone-producing algae to the total amount of suspended particles. *Ohkouchi et al.* [2002] explained the age offset between foraminifera and alkenones at the Bermuda Rise with lateral transport of alkenones on fine-grained particles from the Nova Scotian margin. *Sachs and Anderson* [2003] found Holocene temperatures 4° to 6°C higher than expected in drift sediments of the southern Cape Basin and ascribed this deviation to lateral advection of alkenones that were produced in warmer surface waters to the north. *Müller and Fischer* [2004] observed anomalously high alkenone temperatures in samples taken from a sediment trap deployed in the central tropical Atlantic. They assume this temperature deviation was caused by particles originating from the warmer western equatorial Atlantic and drifting several hundreds of kilometers eastward with the South Equatorial Undercurrent. *Sicre et al.* [2005] suggest that exceptionally high glacial alkenone tem-

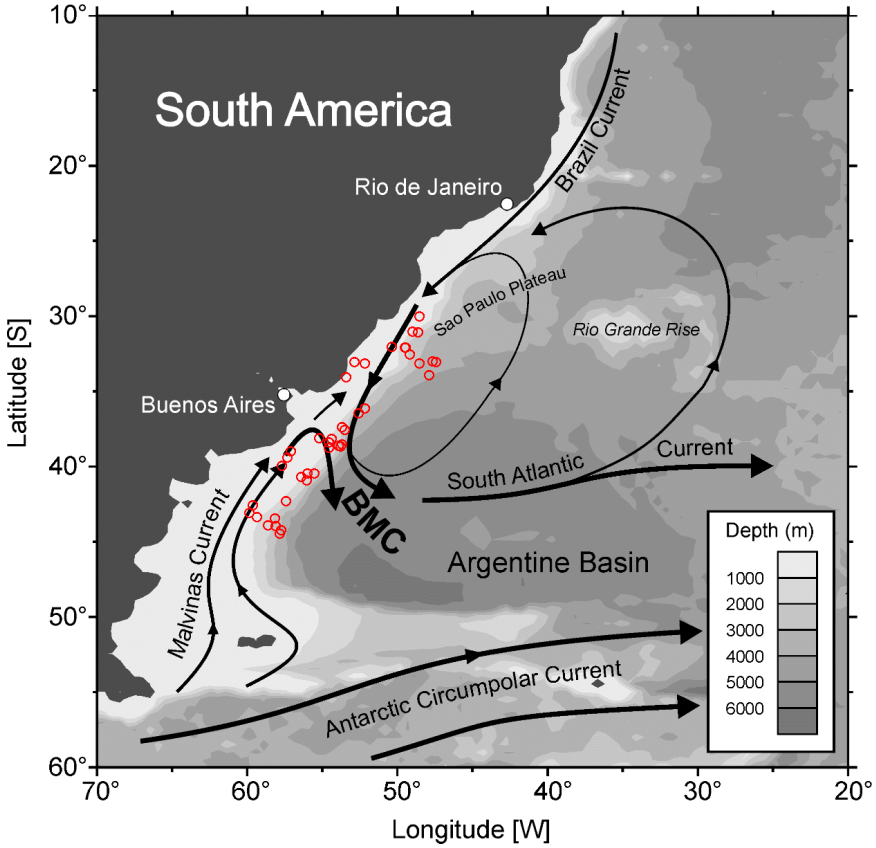

Figure 2. Bathymetric map of the Argentine Basin (modified after *Benthien and Müller*, [2000]) showing the general surface circulation pattern after *Peterson and Stramma* [1991] and the locations of surface water samples taken for the analysis of suspended particulate organic material in February/March 2001.

peratures in the Indian Southern Ocean result from the southeastward advection of organic detritus with the Agulhas Current retroflection. These examples highlight the possible influence of lateral transport of detrital alkenones on the interpretation of local $U^{K'}_{37}$ signals as proxies for modern and past environmental conditions.

[5] To further assess the causes of $U^{K'}_{37}$ temperature anomalies in the Argentine Basin, we have filtered the suspended particulate matter from 53 surface water samples collected along the South American continental margin (Figure 2). Our results suggest that anomalously low alkenone temperatures in the southern BMC area are caused by northward advection of particles with the cold surface waters of the Malvinas Current. In contrast, slightly positive temperature anomalies north of the BMC probably derive from the southward transport of organic detritus with the warm Brazil Current which originates in the western tropical Atlantic. Experiments with the LSG ocean circulation model exemplify other areas of the world ocean where lateral particle advection may significantly bias alkenone temperature data.

2. Material and Methods

2.1. Alkenones From Suspended Particulate Matter

[6] Suspended particulate matter was collected from surface waters of the Argentine Basin during two cruises with the Research Vessel METEOR (M49/2, 13 February to 7 March 2001, and M49/3, 9 March to 1 April 2001) between 30° and 45°S (Figure 2). Eighty-four to one thousand liters of water were obtained directly from the ship's clean seawater intake (~5 m water depth) and pumped through glass fiber filters (Whatman GF/F, nominal pore size 0.7 μm). Before use, the filters were heated at 400°C for 18 h to remove organic compounds. After filtering, all samples were frozen immediately and stored at −18°C until analysis. Temperatures and salinities derive from the vessel's

thermosalinograph. In addition, two deep water samples of 180 liters each were taken in January 2000 (METEOR cruise M46/3) approximately 5 meters above seafloor at water depths of 510 m and 2830 m with a carousel water sampler (Hydro-Bios), which was equipped with 18 Niskin bottles and conductivity, temperature, and depth sensors (Sea-Bird Electronics SBE-19).

[7] After freeze-drying, the filters were cut into small pieces, mixed with an internal standard (squalane; $C_{30}H_{62}$), and the organic material was extracted with a mixture of successively less polar, twice-distilled methanol and methylene chloride (CH_3OH, CH_3OH/CH_2Cl_2 1:1, CH_2Cl_2) by ultrasonication using a UP 200H sonic disruptor probe (Hielscher GmbH, 200 W, amplitude 105 mm, pulse 0.5 s) for 3 min. After each extraction the suspensions were centrifuged and the supernatants combined, desalted with deionized water, dried with preheated Na_2SO_4, and rotary evaporated to dryness. The residues were redissolved in 100 μl of CH_2Cl_2 and cleaned by elution (3 $\times$ 500 μl CH_2Cl_2) through a commercial silica cartridge (silica Bond Elute SPE column, Varian). To eliminate possibly coeluting fatty acid methyl esters, the clean extracts were hydrolyzed with 300 μL of 0.1 M KOH in 90/10 CH_3OH/H_2O at 80°C for 2 h. The neutral fraction containing the alkenones was obtained by partitioning into hexane (3 $\times$ 500 μL). Finally, the extracts were concentrated under N_2 and taken up in 25 μl of a $MeOH/CH_2Cl_2$ mixture. The extracts were analyzed by gas chromatography using a HP 5890 series II gas chromatograph equipped with a 50 m fused silica capillary column (HP Ultra 1, 0.32 mm $\times$ 0.52 μm), split/splitless injection (1:10), and a flame ionization detector (with helium as carrier gas). The injector and detector temperatures were 280° and 320°C, respectively. The oven temperature was programmed to give 50°–150°C at 30°C min^{-1}, 150°–230°C at 8°C min^{-1}, and 230°–320°C at 6°C min^{-1} and the final temperature maintained for 45 min. Analytical precision ($\pm 1\sigma$), based on multiple extractions of a sediment used as a laboratory-internal reference sample, was better than 0.01 units (or 0.3°C). We determined the alkenone unsaturation index $U^{K'}_{37}$ and converted it into temperature using the global calibrations of *Müller et al.* [1998] based on core top sediments (equation (1)) and *Conte et al.* [2006] based on sea surface suspended particulate material (equation (2)).

$$T = \left(U^{K'}_{37} - 0.044\right)/0.033 \quad (1)$$

$$T = -0.957 + 54.3\left(U^{K'}_{37}\right) - 52.9\left(U^{K'}_{37}\right)^2 + 28.3\left(U^{K'}_{37}\right)^3 \quad (2)$$

[8] For comparison with the temperature anomalies computed from LSG model simulations, we compiled a data set of all the $U^{K'}_{37}$ data deriving from surface water particles collected at water depths <10 m from the literature as well as our own data from the Atlantic, Pacific, and Indian oceans. This compilation comprises 418 individual sites, many of which are located along continental margins. A complete list of sampling sites used here can be found on the PANGAEA data archive http://www.pangaea.de/home/cruehlemann). It includes data published by *Conte and Eglinton* [1993], *Sikes and Volkman* [1993], *Conte et al.* [1994, 2006], *Ternois et al.* [1997], *Sawada et al.* [1998], *Bentaleb et al.* [1999, 2002], *Cacho et al.* [1999], *Shin et al.* [2002], *Harada et al.* [2003], *Bac et al.* [2003], *Bendle and Rosell-Melé* [2004], and *Prahl et al.* [2005]. We interpolated the data using variogram analysis and ordinary kriging [*Davis*, 1986]. On the basis of the $U^{K'}_{37}$ dataset, we generated 2.5° $\times$ 2.5° grids of deviations (ΔSST) between the global $U^{K'}_{37}$ temperature data obtained on surface seawater POM (according to the *Conte et al.*'s [2006] calibration; equation (2)) and the respective water temperatures measured at sampling depths for each of the four seasons:

$$\Delta SST[^\circ C] = SST\left(U^{K'}_{37\ POM}\right) - SST(measured) \quad (3)$$

The search radius for calculating the grid was restricted to 7° in latitude and longitude in order to avoid unreasonably long distances for interpolation.

2.2. Model Setup and Experimental Design

[9] To investigate the effect of long residence times and lateral transport of sea surface suspended particles on ΔSST, we used an improved version of the Hamburg LSG ocean circulation model [*Maier-Reimer et al.*, 1993] in which the original upstream advection scheme for temperature, salinity and other tracers has been replaced by a less diffusive third-order QUICK scheme [*Schäfer-Neth and Paul*, 2001]. The model has a horizontal resolution of 3.5° $\times$ 3.5° on an E grid and 22 irregularly spaced levels, with a surface layer thickness of 50 m. The ocean is forced by 10-year averaged monthly fields of wind stress, surface air temperature, and freshwater flux, which originate from present-day climate simulations with the atmosphere general circulation model ECHAM3/T42.

A surface heat flux formulation based on an atmospheric energy balance model with diffusive lateral heat transports permits that sea surface temperatures (SST) can freely adjust to changes in the ocean circulation [e.g., see *Prange et al.*, 2003]. The hydrological cycle is closed by a scheme for continental runoff in which precipitation over continental catchment areas is discharged to the oceans following the steepest gradient of the model topography. In the model, sea surface salinities can freely evolve. Our model reproduces the observed distributions of temperature, salinity and radiocarbon for the present day within reasonable error margins [*Butzin et al.*, 2005].

[10] The apparent temperature deviation in a water sample was estimated from Lagrangian tracking of its pathway through the surface layer, which is given by

$$r(t) = r(t_0) + \int_{t_0}^{t} \boldsymbol{u}(\boldsymbol{r}, t')\mathrm{d}t', \tag{4}$$

where $\boldsymbol{r}$ is the displacement of the water parcel at times t and t_0, respectively, and $\boldsymbol{u}$ is the velocity. The SST difference ΔT along a streamline is

$$\Delta T = T(r(t_0), t_0) - T(r(t), t), \tag{5}$$

where T denotes the local (Eulerian) sea surface temperatures at the beginning and end of the calculation, respectively. Positive values of ΔT signify cooling of a water parcel during its journey, which implies that suspended alkenones may carry a higher temperature signal than actually displayed by thermometer measurements. In a global analysis using seasonal (i.e., 3 months) SSTs and surface velocity fields (averaged over 10 years), we calculated ΔT for 90 and 180 days of lateral advection. As a result we obtained global maps of ΔT with which, for a given season and place, the temperature effect of different advection histories can be estimated. However, the marine biosphere is not represented in our model, leading to simulations which strongly simplify the complex natural cycle of biological production as we consider only the transport of nonliving organic particles produced at a certain point of time and neglect mixing with alkenones from subsequent coccolithophore production along its pathway. Observations from culture experiments demonstrate that coccolithophores adjust their alkenone unsaturation to changes in growth temperature on a timescale of days [*Prahl et al.*, 1988; *Conte et al.*, 1998]. So, if deviations between alkenone temperatures determined from surface water particles and in situ temperatures are predominantly caused by long particle residence times and lateral transport, then the amount of alkenones originating from dead organic material must largely outweigh the amount of alkenones derived from living algae. Indeed, it is generally thought that nonliving POM (detritus) exceeds that of plankton by 10:1, although their relative abundances may significantly vary in space and time [*Volkman and Tanoue*, 2002]. Therefore our model experiments represent a valid approach for a first-order estimate of the influence of lateral transport of POM on alkenone temperature signals.

3. Oceanographic Setting

[11] The upper level circulation in the Argentine Basin is dominated by the Brazil and Malvinas (Falkland) Currents [*Peterson and Stramma*, 1991] (Figure 2). The Brazil Current is a western boundary current carrying warm and salty subtropical water poleward along the continental margin of South America (Figure 2). Surface velocities range between 30 and 80 cm s^{-1}, strengthening at southern latitudes under the influence of a recirculation cell [*Peterson and Stramma*, 1991; *Vigan et al.*, 2000]. Surface temperatures in the Brazil Current are 24° to 28°C during summer and 20°C during winter. At about 38°S the Brazil Current encounters the Malvinas Current, which originates as a branch of the Antarctic Circumpolar Current east of the Drake Passage and transports cool (surface temperatures of 4° to 5°C during winter and 9° to 11°C during summer), less saline, nutrient-rich subantarctic water equatorward along the Argentine continental shelf [*Vivier and Provost*, 1999; *Vigan et al.*, 2000]. As this strong current flows northward, it is rapidly warmed by mixing and heat gain [*Provost et al.*, 1996]. Direct velocity measurements of the surface Malvinas Current are scarce. According to *Peterson et al.* [1996], drifters deployed at 100 m depth in the core of the northward flowing Malvinas Current traveled at velocities between 60 and 80 cm s^{-1} and were in excess of 100 cm s^{-1} in the southward and westward directed Brazil–Malvinas return flow. The frontal zone between the water masses of the Brazil and Malvinas Currents generates the Brazil-Malvinas Confluence, which is characterized by sharp horizontal gradients in temperature (reaching up to 1°C km^{-1}), salinity, and nutrients [*Olson et al.*, 1988; *Bianchi et al.*, 1993; *Provost et al.*, 1995; *Goni et al.*, 1996; *Brandini et al.*, 2000]. The

region shows a complex and variable mesoscale circulation pattern associated with intense mixing and the generation of meanders and eddies, in which SST anomalies can be up to 10°C over a period of about two months [*Piola and Matano*, 2001]. Furthermore, hydrographic measurements from high spatial resolution surveys at the BMC reveal a complex vertical thermohaline structure of interleaving subantarctic and subtropical waters, featuring intrusions which sometimes form layering of relatively cold and fresh water over warmer and saltier water within the upper 100 m [*Bianchi et al.*, 1993]. These processes can lead to a vertical density structure in the surface layer that precludes sinking of phytoplankton cells.

[12] The biology of the BMC is characterized by an admixture of subtropical and subantarctic organisms [*Boltovskoy et al.*, 1996]. Primary productivity is generally lower in the warm oligotrophic waters of the Brazil Current than in the nutrient-rich Malvinas Current (Figure 3a). Satellite images reveal coccolithophore blooms in the southwestern Atlantic occurring episodically throughout the year with maxima from late austral spring to summer [*Brown and Podestá*, 1997]. On the basis of spectral signature estimation, *Brown and Podestá* [1997] concluded that these blooms are predominantly caused by *E. huxleyi*. High concentrations of phytoplankton have particularly been observed along the shelf break and slope from off the Río de la Plata to south of the Malvinas Islands. These phytoplankton blooms are likely due to enhanced nutrient concentration resulting from upwelling

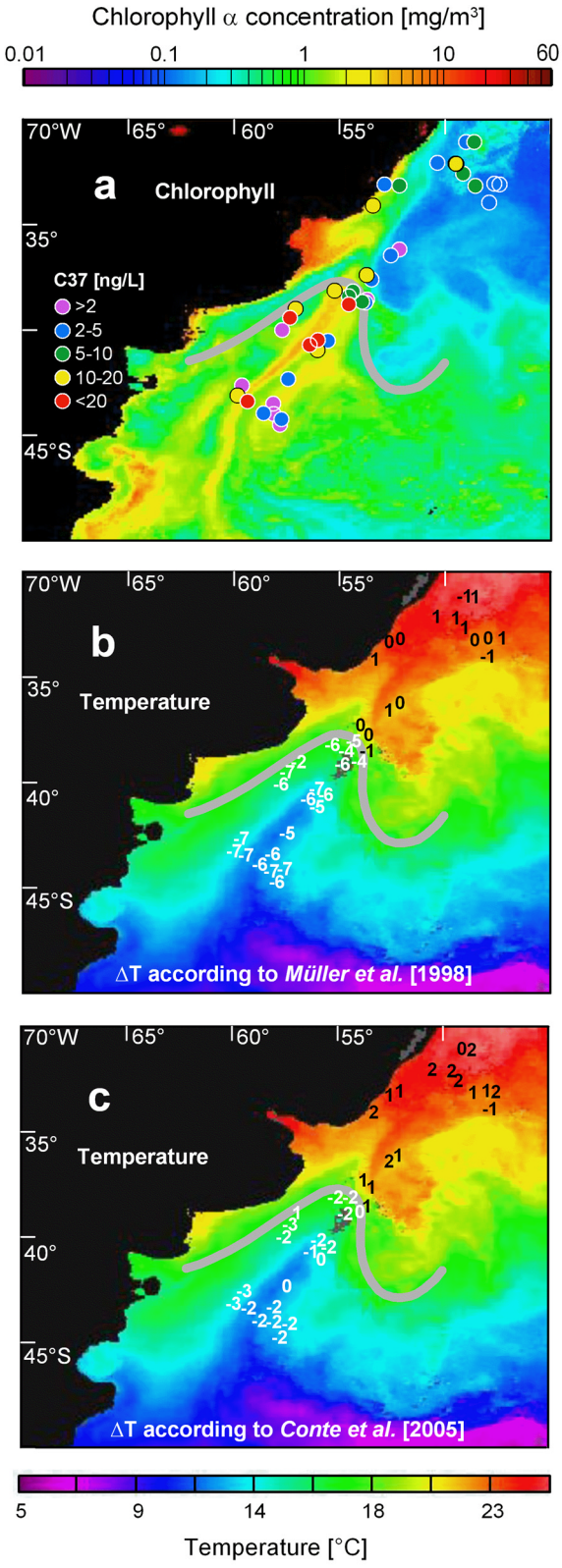

Figure 3. Alkenone concentrations and temperature anomalies compared to (a) satellite-derived chlorophyll concentrations and (b, c) sea surface temperatures for February 2001, respectively. Numbers in Figures 3b and 3c represent differences (°C) between $U^{K'}_{37}$ temperatures obtained from suspended particulate organic matter (collected from 5 m water depth in February/March 2001) and water temperatures measured at sampling depth. The $U^{K'}_{37}$ ratios were converted to temperatures using the global core top calibrations of *Müller et al.* [1998] in Figure 3b and those of *Conte et al.* [2006] in Figure 3c. Numbers display sampling locations (where samples were located too close to each other, we slightly shifted the position of the numbers to avoid overlapping). Positive values indicate that $U^{K'}_{37}$ temperatures were warmer than in situ temperatures. The thick gray line signifies the 18°C isotherm which approximately coincides with the Brazil-Malvinas Confluence [*Brandini et al.*, 2000]. Satellite SSTs (Pathfinder 4, nighttime data) and chlorophyll concentrations (SeaWiFS) are monthly averages for February 2001. Data were obtained from the SeaWiFS project http://seawifs.gsfc.nasa.gov/cgi/level3.pl) and the Jet Propulsion Laboratory http://poet.jpl.nasa.gov), respectively.

[*Carreto et al.*, 1995]. *E. huxleyi* occurred in November-December 1989 off the Río de la Plata from the surface to 75 m water depth with maximum cell concentrations at 25 m [*Gayoso*, 1995]. This agrees with results of *Brandini et al.* [2000], who reported highest chlorophyll α concentrations in the upper 25 m of the water column of the Brazil-Malvinas Confluence region at the beginning of the austral summers of 1993 to 1995.

4. Results and Discussion

4.1. Alkenone Temperature Anomalies in the Brazil-Malvinas Confluence Area

[13] *Benthien and Müller* [2000] showed that the alkenone $U^{K'}_{37}$ in core top sediments recovered from the Argentine Basin deviates significantly from that predicted by the *Müller et al.* [1998] core top calibration. However, the sedimentary alkenone signal at mid to high latitudes, and thus the global calibration of *Müller et al.* [1998] based on core tops, seems to be biased by seasonality in production, as primary productivity tends to shift to the warmer season with increasing distance from the tropics [*Conte et al.*, 2006]. In order to enable comparison to the *Benthien and Müller* [2000] results, we have used the *Müller et al.* [1998] calibration to convert the $U^{K'}_{37}$ data from the Argentine Basin into temperature, but also show the results for the *Conte et al.* [2006] calibration.

[14] In Figure 3, we compare alkenone temperature anomalies to satellite-derived chlorophyll concentrations and sea surface temperatures for February 2001. Alkenone temperatures for surface waters determined from samples taken south of the BMC (approximated by the 18°C isotherm, thick gray line) are 4° to 7°C lower than measured water temperatures when using the *Müller et al.* [1998] calibration (Figure 3b and Table 1). In contrast, alkenone temperatures determined from samples taken north of the confluence agree with thermometer values or are slightly higher by up to 1°C, except for two locations in the north of the study area and one sample from the confluence region. Using the *Conte et al.* [2006] calibration, temperature anomalies south of the BMC predominantly range between −2 and −3°C whereas $U^{K'}_{37}$ temperatures north of the BMC are 1° to 2° C higher than measured water temperatures (Figure 3c).

[15] Alkenone concentrations ($C_{37:2}$ + $C_{37:3}$) in surface waters of the Argentine Basin are similar in magnitude to those observed in other ocean areas [e.g., *Conte and Eglinton*, 1993; *Sikes et al.*, 1997; *Sikes and Sicre*, 2002; *Bendle and Rosell-Melé*, 2004] and range from 2.0 to 15.6 ng/L (average of 19 values: 6.3 ng/L) north of the BMC and from 0.8 to 56.5 ng/L (average of 23 values: 12.4 ng/L) south of the confluence area, respectively. Highest concentrations occur along the shelf break and slope south of the BMC and in the confluence region with the Brazil Current (Figure 3a). These results confirm the observations from satellite images that chlorophyll concentration and coccolithophorid production [*Brown and Podestá*, 1997] are generally enhanced in the Malvinas Current compared to the Brazil Current and are highest along the shelf break. However, sampling locations with high or low alkenone concentrations occur closely together and do not strictly coincide with high or low SeaWiFS chlorophyll concentrations, respectively. The bottom water samples did not contain detectable amounts of alkenones (detection limit of ~1 ng per compound).

4.2. Causes of the Alkenone Temperature Anomalies in the Brazil-Malvinas Confluence Area

[16] Three alternative factors may account for the anomalously low alkenone temperatures south of the BMC: (1) the predominance of alkenone-producing algal species which do not match the $U^{K'}_{37}$ -temperature relationships determined by *Müller et al.* [1998] and *Conte et al.* [2006], (2) physiological factors such as nutrient availability and growth rate, and/or (3) long residence times and lateral transport of suspended particles in the surface water which may lead to differences between actual growth temperature recorded by the algae and the water temperature from where the samples were collected.

4.2.1. Species Dependence, Nutrient Availability, and Growth Rate

[17] Recent results from culture experiments have indicated that alkenone-derived temperatures may be affected by biological and environmental factors such as genetic differences between haptophyte species and within given species isolated from different oceanic regimes [*Volkman et al.*, 1995; *Sawada et al.*, 1996; *Conte et al.*, 1998], as well as variations in nutrient availability [*Epstein et al.*, 1998] and growth rate [*Popp et al.*, 1998]. On the basis of culture experiments, *Popp et al.* [1998] deduced a small decrease in $U^{K'}_{37}$ from 0.33 to 0.27 with increasing growth rates (0.2 to 0.6 d^{-1}) for a

Table 1. Station Data and Analytical Results for Filter Samples Obtained During Meteor Cruises M49/2 and M49/3

Latitude, °S	Longitude, °W	Date (2001)[a]	Volume Filtered, L	Temperature, °C	Salinity, psu	C37:3, ng L^{-1}	C37:2, ng L^{-1}	$U_{37}^{K'}$
39.00	57.08	14.02.	390	18.3	33.6	6.0	8.0	0.573
39.42	57.34	14.02.	330	18.2	33.6	15.6	10.3	0.397
40.00	57.71	14.02.	650	17.4	33.8	0.7	0.5	0.426
42.63	59.63	15.02.	1000	15.6	33.7	0.8	0.4	0.311
43.10	59.84	15.02.	650	15.3	33.8	12.6	5.8	0.317
43.39	59.36	15.02.	305	13.7	33.9	38.8	14.6	0.275
44.25	57.75	16.02.	400	13.6	34.1	2.0	0.7	0.274
43.95	58.60	17.02.	370	13.5	34.1	2.3	0.9	0.282
43.99	58.12	18.02.	410	13.4	34.1	1.1	0.4	0.268
44.51	57.82	20.02.	516	13.2	34.1	1.3	0.5	0.272
43.51	58.14	21.02.	460	13.3	34.1	0.6	0.2	0.274
42.34	57.44	22.02.	410	12.6	34.1	3.3	1.5	0.311
40.51	55.55	23.02.	523	14.0	34.1	1.6	0.7	0.293
40.49	56.01	24.02.	400	13.0	33.7	15.1	5.2	0.256
40.71	56.42	25.02.	340	12.8	33.9	40.1	15.4	0.277
40.97	56.04	26.02.	573	11.8	34.0	8.2	3.2	0.279
38.79	54.57	27.02.	950	15.3	33.8	13.4	7.1	0.344
38.56	53.69	28.02.	500	20.7	32.8	0.5	1.0	0.682
38.70	53.76	28.02.	110	19.1	33.8	1.2	1.6	0.565
38.66	53.92	28.02.	84	17.9	33.8	3.6	3.6	0.503
38.40	54.56	28.02.	121	17.9	33.7	2.5	2.2	0.462
38.13	55.23	28.02.	87	17.0	33.7	10.3	7.3	0.414
38.17	54.35	28.02.	92	18.7	33.8	5.1	4.8	0.483
37.39	53.71	01.03.	208	23.3	29.5	2.3	10.3	0.816
37.60	53.49	02.03.	280	23.4	34.2	0.6	2.5	0.818
38.40	54.56	03.03.	131	19.4	33.8	3.4	4.4	0.568
36.47	52.57	04.03.	441	22.4	35.5	0.9	3.8	0.801
36.18	52.17	05.03.	210	24.6	30.9	0.3	1.7	0.865
34.08	53.42	10.03.	39	23.5	31.5	2.2	13.4	0.859
33.08	52.86	10.03.	251	25.4	31.4	0.3	2.1	0.891
33.14	52.16	10.03.	332	26.4	33.0	0.4	5.3	0.924
32.06	50.37	11.03.	273	27.0	35.9	0.1	3.3	0.976
32.12	49.45	11.03.	248	26.8	36.2	0.5	14.0	0.965
33.06	47.65	12.03.	324	24.6	35.9	0.6	3.8	0.863
33.08	47.41	12.03.	391	25.9	36.2	0.3	4.5	0.938
31.08	48.61	13.03.	594	26.6	36.7	0.3	8.6	0.965
33.95	47.90	14.03.	382	25.4	36.0	0.4	2.0	0.833
31.07	49.00	14.03.	416	25.9	36.1	0.3	2.1	0.873
32.10	49.50	15.03.	192	26.9	36.1	0.2	10.5	0.978
33.16	48.55	15.03.	707	26.9	36.4	0.3	5.1	0.944
32.58	49.15	16.03.	544	26.8	36.0	0.2	6.2	0.966
30.06	48.51	18.03.	365	27.0	35.8	0.1	3.6	0.981
29.06	43.50	19.03.	372	27.5	36.5	0.1	1.3	0.920
27.06	41.89	20.03.	416	27.9	36.6	0.5	4.4	0.896
26.07	43.56	21.03.	299	28.3	36.8	0.1	1.6	0.952
25.08	44.67	22.03.	263	27.6	37.0	0.1	3.2	0.985
24.02	44.52	24.03.	292	28.0	37.1	0.1	2.5	0.977
26.01	43.55	25.03.	494	28.8	36.7	0.1	1.4	0.944
26.07	43.45	26.03.	379	28.3	36.8	0.1	1.4	0.944
27.11	42.42	28.03.	655	28.1	36.8	0.1	2.3	0.951
24.04	40.66	29.03.	442	28.2	36.8	0.1	1.8	0.963
19.60	38.61	30.03.	475	28.9	37.3	0.0	1.4	0.972
16.59	38.27	31.03.	744	28.9	37.1	0.0	2.8	0.986

[a] Read 14.02. as 14 February.

noncalcifying strain of *E. huxleyi*, although experiments with two calcifying strains of *E. huxleyi* (probably the dominant varieties in the BMC region) revealed no systematic variations between $U_{37}^{K'}$ and growth rate [*Popp et al.*, 1998; *Riebesell et al.*, 2000]. In the Malvinas Current region, nutrient levels in surface waters are generally higher than in the less productive Brazil Current

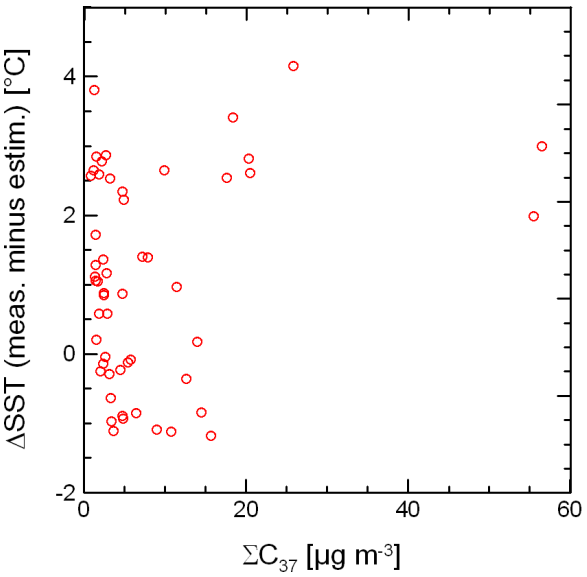

Figure 4. Scatterplot of alkenone temperature anomalies (measured minus estimated) against the sum of C_{37} alkenone concentrations in surface waters of the Brazil-Malvinas Confluence. The $U^{K'}_{37}$ data were converted to temperature using the calibration of *Conte et al.* [2006].

[*Brandini et al.*, 2000] and the anomalously low $U^{K'}_{37}$ values south of the BMC could therefore at least partly be due to higher nutrient availability and enhanced algal growth rates. However, a decrease in $U^{K'}_{37}$ from 0.33 to 0.27 would be equivalent to a temperature drop of ~2°C; not enough to explain the temperature anomalies of up to −7°C south of the BMC and even counteracting the positive anomalies north of the BMC. Moreover, in our dataset, the alkenone temperature anomalies show no correlation with alkenone concentrations (Figure 4) and we also do not observe negative temperature anomalies in the high chlorophyll areas north of the Río de la Plata mouth (Figure 3a), which would be expected if nutrient-limited growth rate were a major factor controlling the $U^{K'}_{37}$.

[18] The differences in temperature anomalies north and south of the BMC could also be due to different coccolithophorid species prevailing in the subtropical and subantarctic waters, respectively. For example, several culture experiments using *G. oceanica* have revealed significant differences in the $U^{K'}_{37}$ /temperature relationship of this species [*Volkmann et al.*, 1995; *Sawada et al.*, 1996; *Conte et al.*, 1998]. However, in the studied area this possibility seems very unlikely as the predominance of calcifying *E. huxleyi* in both the waters of the Malvinas Current and the Brazil Current is indicated by satellite mapping for the austral summers 1978–1979 to 1985–1986 [*Brown and Podestá*, 1997]. In situ samples collected along the shelf break in the western South Atlantic also generally confirm the dominance of *E. huxleyi* during austral spring and summer [*Hentschel*, 1936; *Gayoso*, 1995]. Moreover, *G. oceanica* predominantly occurs in warm marginal seas [*Okada and Honjo*, 1975] and in boundary regions of low latitudes [*Andruleit et al.*, 2004] whereas it is less abundant in cold subantarctic waters. Hence the information available suggests that *E. huxleyi* is the dominant species in the BMC region. Furthermore, the observed universality of the *Conte et al.* [2006] temperature calibration based on sea surface suspended particles indicates that genetic and growth factors introduce minimal temperature bias. Their global compilation of data from the Pacific, Indian and Southern Oceans exhibits a remarkable degree of agreement considering the diversity of environments sampled. In fact, there is excellent agreement between samples in which *Gephyrocapsa* spp. is the major alkenone synthesizer (e.g., in the western Pacific) and samples from regions where *E. huxleyi* prevails. This agreement clearly does not support the suggestion that *Gephyrocapsa* spp. is different from *E. huxleyi* regarding its alkenone versus growth/temperature relationship.

4.2.2. Lateral Particle Transport

[19] The above considerations imply that the anomalous $U^{K'}_{37}$ values observed in the western Argentine Basin cannot be convincingly explained by biological processes. We therefore favor lateral advection of the detritus of alkenone-producing algae within the Malvinas Current and the Brazil Current to explain the discrepancies between reconstructed and measured surface water temperatures. Particles in the ocean occur as a continuum of sizes, showing an exponential increase in the number of particles per volume of water with decreasing size [*McCave*, 1975]. Turbulence in the mixed layer counteracts the tendency of particles to settle out of suspension. Smaller particles (<20 μm) may thus remain suspended in surface waters for weeks or even months and drift with ocean currents until they can sink to depth through particle aggregation, usually during the terminal stages of blooms [*Eppley et al.*, 1983]. *Moran and Smith* [2000] used ^{234}Th activities to calculate particle residence times of ~10 to 50 days in the upper 50 m of the Beaufort Sea in the Arctic Ocean. *Schmidt et al.* [2002a, 2002b] applied the

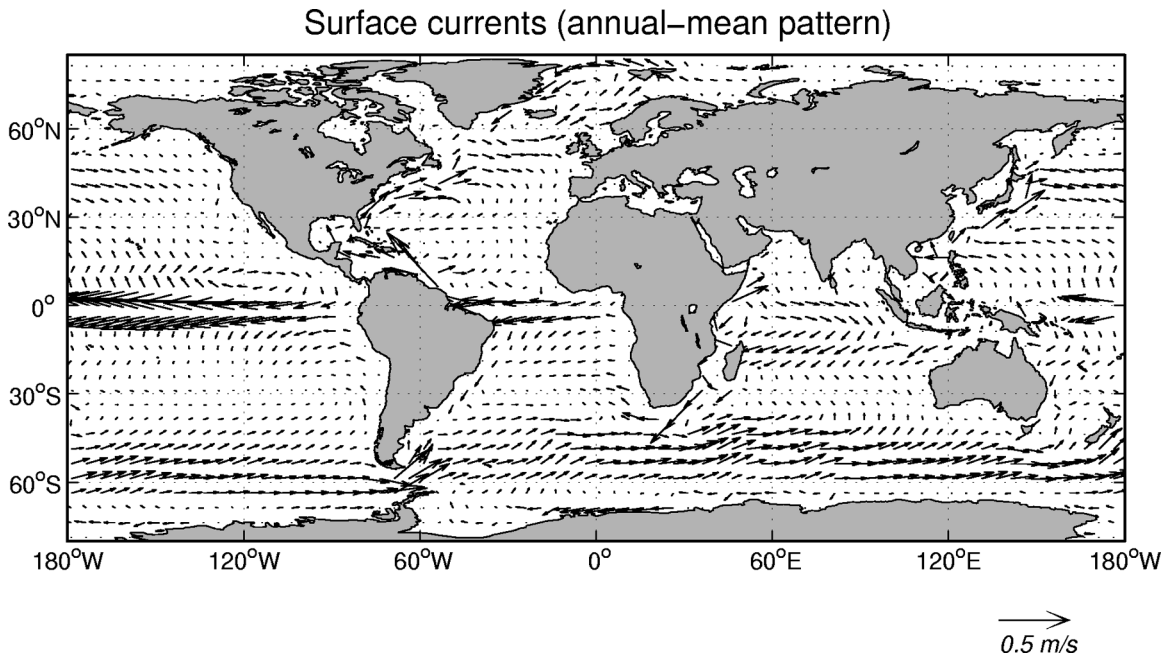

Figure 5. Annual mean surface flow simulated with the LSG ocean circulation model. Current vectors are shown for every second grid point only.

same technique and determined average particle residence times of 26 days in June (preupwelling season) and 113 days in January (low productivity season) in surface waters off northwest Portugal, and values ranging between <10 and >250 days (depending on the trophic conditions and plankton production rates) in the northwestern Mediterranean Sea. Long residence times of suspended particles in the northwestern Mediterranean Sea, where alkenones are produced at the end of fall and can be retained in the surface water until winter, have also been suggested by *Sicre et al.* [1999]. *Eppley et al.* [1983] estimated the residence time for particulate organic carbon in the surface layer of the Southern California Bight and the central North Pacific between 3 and >100 days. Regarding these examples for particle residence times in various ocean areas, it is reasonable to assume that a significant portion of the alkenones produced remains in the ocean surface layer for some time and is possibly advected over long distances.

[20] We thus suggest that the temperature anomalies found in the northern Malvinas Current are caused by the northward transport of allochthonous alkenones carrying a cold water signal and masking the autochthonous molecular signal. In particular, the close distance between samples showing anomalously low temperatures and samples that almost perfectly match in situ values at the BMC (Figures 3b and 3c) strongly supports the assumption that lateral transport is the main cause of the discrepancies between alkenone and sea surface temperatures in the Malvinas Current. Our assumption agrees with other studies showing that planktic organisms such as diatoms [*Jones and Johnson*, 1984] and even foraminifera [*Boltovskoy*, 1994; *Boltovskoy et al.*, 1996] are likewise displaced equatorward over long distances in the Argentine Basin. The surface water pattern of anomalously low temperatures apparent in our data is mirrored in the surface sediments of the BMC region [*Benthien and Müller*, 2000], indicating that transport of southern-derived particles in the upper water column is the predominant factor responsible for the deviating $U^{K'}_{37}$ temperatures in core top samples from the Argentine Basin. This conclusion is corroborated by results of *Mollenhauer et al.* [2006], who found similar radiocarbon ages for alkenones and co-occurring planktic foraminifera in the same surface sediments from the Argentine Basin as were analyzed by *Benthien and Müller* [2000]. From the apparently coeval deposition of these sediment constituents they inferred that the transport processes must be due to rapid advection in the upper water column. Further evidence for the predominant transport of southern source alkenone detritus in surface waters is provided by the appar-

ent lack of alkenones in bottom waters at two stations on the upper and lower continental slope north and south of the BMC, respectively.

4.3. Model Simulations of Temperature Anomalies Caused by Particle Transport

[21] On the basis of surface ocean transport pathways and velocities (Figure 5) which have been simulated with the LSG ocean circulation model, we identify areas of the world ocean where alkenone temperatures could potentially be biased to higher or lower values due to long residence times and the lateral advection of suspended particles. Modeled differences between alkenone and water temperatures caused by particle residence times of 90 days and 180 days are shown in Figures 6 and 7, respectively. Blue (red) colors indicate detrital alkenones carrying a temperature signal that is lower (higher) than in situ water temperatures.

[22] In principle, discrepancies between alkenone and water temperature may result from (1) heat gain or loss caused by mixing of water masses of different temperatures, and (2) changes in seasonal insolation and associated surface water heating or cooling. According to our model results, seasonal variations in insolation cause much larger ΔSSTs than water mass mixing. A noticeable effect by mixing occurs only at oceanic frontal zones after lateral transport of at least 180 days and is restricted to the Nordic Seas, the Agulhas Current region, and the southern Westwind Drift between 40° and 60°S where northeastward transport in the surface layer carries alkenones from subpolar to temperate regions. Figures 6 and 7 illustrate the combined effects of water mass mixing and seasonal insolation changes on ΔSST. In general, seasonal temperature changes of the surface ocean force simulated $U^{K'}_{37}$ temperatures to be higher (lower) than ambient water temperatures when $U^{K'}_{37}$ is determined from samples taken in the first (second) half of the year in the Northern Hemisphere, or the reverse in the Southern Hemisphere. Largest simulated $U^{K'}_{37}$ temperature anomalies occur at mid latitudes around 40° where seasonality in sea surface temperature is largest: off eastern North America, in the Greenland Sea, the Sea of Okhotsk, and the Bering Strait.

[23] The discrepancies between $U^{K'}_{37}$ temperatures obtained from sea surface POM and in situ temperatures calculated for the four seasons (Figure 8) share many similarities with the respective simulations of ΔSST. For instance, samples collected in the Atlantic in December/January/February compare well with the simulations for 180 days of particle residence time whereas the North Pacific samples for this season largely coincide with residence times of 90 days. The ΔSST from samples taken in March/April/May match reasonably well with simulations of 90 days as well as 180 days of particle transport, except for POM collected in the Argentine and Cape Basins. For June/July/August, ΔSST shows similarities with the simulations for particle residence times of 90 days in the western Pacific whereas samples in the Atlantic show a better comparison with residence times of 180 days, except for the northern North Atlantic and the Nordic Seas. Although the simulations predict cold anomalies for most parts of this region, seawater POM collected during the summer months by *Conte and Eglinton* [1993] in the North Atlantic and by *Bendle and Rosell-Melé* [2004] in the Nordic Seas predominantly yields $U^{K'}_{37}$ temperature anomalies which are several degrees higher than measured water temperatures (up to 10°C in the Greenland Sea). The Nordic Seas are characterized by convective overturning in the late winter, as well as by strong interannual and decadal variability of sea ice cover [e.g., *Divine and Dick*, 2006]. Both effects may bias the temperatures determined from filtered particles, but are not adequately captured by our modeling approach. Warm anomalies in the Greenland Sea may also result from a general lack of correlation between $U^{K'}_{37}$ and water temperatures below 8°C in this area, although the reason for this is still unknown [*Bendle and Rosell-Melé*, 2004]. For particles filtered in September/October/November most samples match the simulations of 90 days as well as 180 days of particle transport. Just off northeastern Africa we observe warm anomalies rather than the cold anomalies expected from the simulations for particle residence times of 90 as well as 180 days, possibly because upwelling of cool water masses masks the signal of seasonal temperature change. Moreover, in upwelling areas, the proportion of living to detrital alkenones is higher and particle residence times are shorter than in the oligotrophic ocean. In summary, there is a good general agreement between ΔSST of the surface seawater POM and of the model simulations for most of the seasons and ocean areas, supporting the assumption that detrital alkenones which remain suspended in surface waters and are possibly advected over long distances can significantly bias the in situ alkenone temperature signal, especially in ocean areas with strong surface

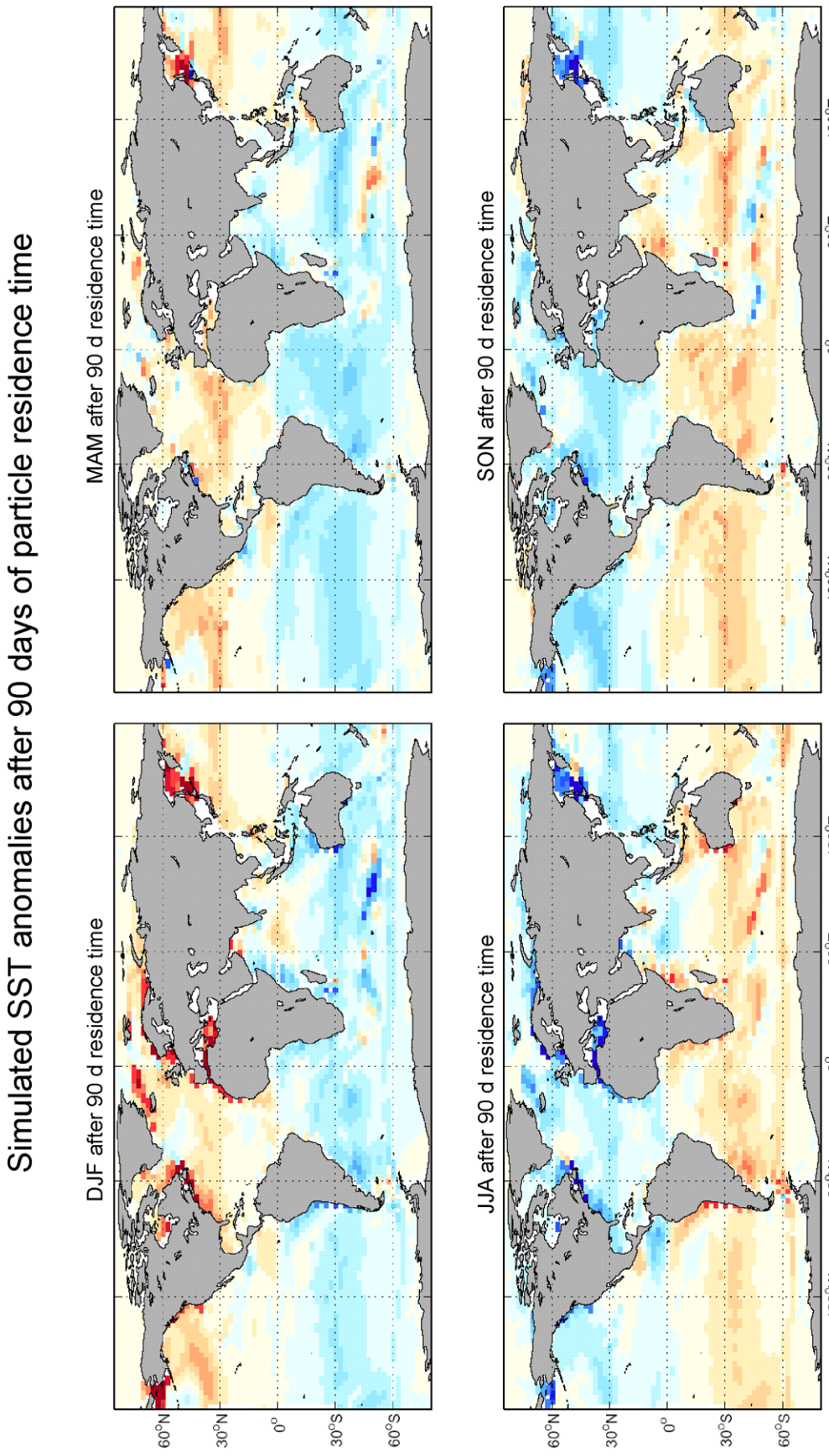

Figure 6. Simulated SST anomalies after 90 days of particle residence time and lateral transport within the ocean surface layer for each of the four seasons. Each panel shows the temperature differences between places of origin and final positions for particles transported in surface waters. Blue (red) colors indicate that particles originate from colder (warmer) surface waters.

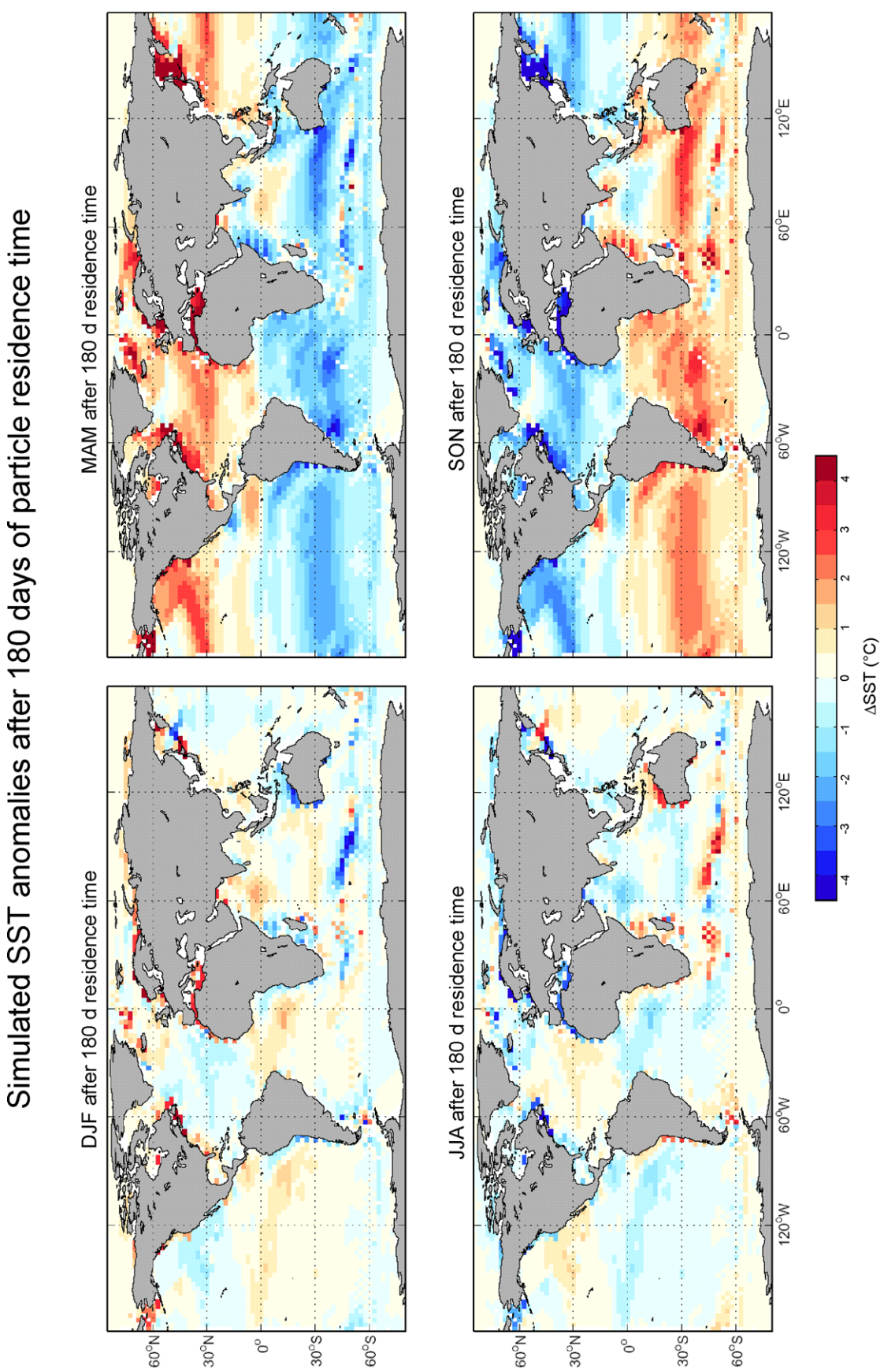

Figure 7. Simulated SST anomalies after 180 days of particle residence time and lateral transport within the ocean surface layer for each of the four seasons. Each panel shows the temperature differences between places of origin and final positions for particles transported in surface waters. Blue (red) colors indicate that particles originate from colder (warmer) surface waters.

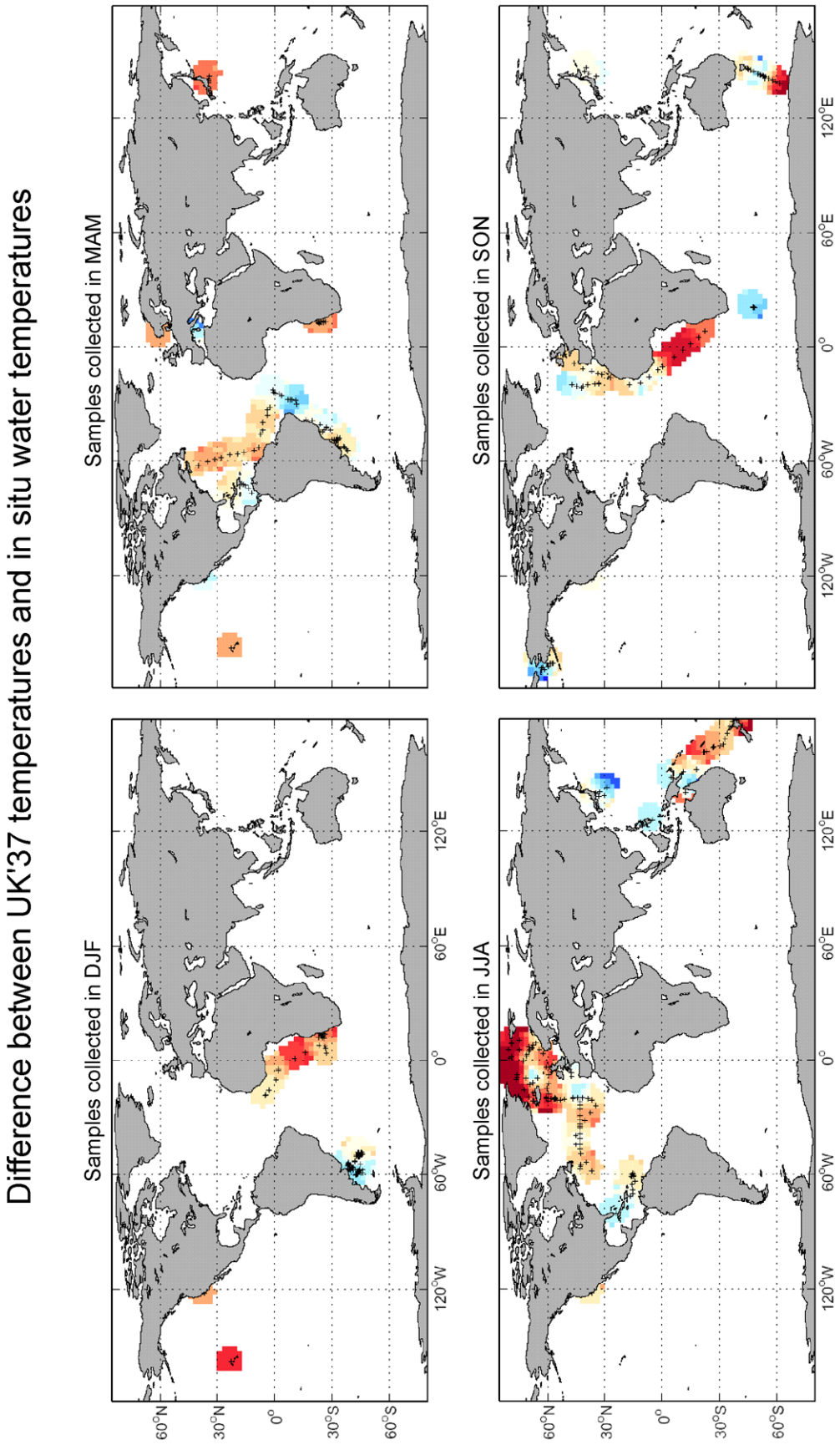

Figure 8. Alkenone temperature anomalies ($U^{K'}_{37}$ temperature minus measured water temperature) determined from suspended particulate organic matter and shown for each of the four seasons. The $U^{K'}_{37}$ ratios were converted to temperature using the calibration of *Conte et al.* [2006]. Black crosses denote sampling positions. Data were interpolated to a 2.5° × 2.5° grid.

current systems and/or extreme productivity and temperature gradients.

5. Conclusions

[24] Our study demonstrates that the anomalously low alkenone temperatures found in surface sediments of the Argentine Basin [*Benthien and Müller*, 2000] can be largely explained by suspended particles drifting with surface currents. The clear resemblance between surface water temperature anomalies and those of the surface sediments [*Benthien and Müller*, 2000] implies that past latitudinal shifts of the Brazil-Malvinas Confluence could be reconstructed from down-core sediment records. The good correspondence in many cases between ΔSST of samples and of simulations suggests that long residence times and transport of particles within the surface layer of the oceans account for a large part of the variability in $U^{K'}_{37}$/temperature data based on both suspended particles and core top sediments [e.g., *Sikes et al.*, 1991; *Sikes and Volkman*, 1993; *Rosell-Melé et al.*, 1995; *Müller et al.*, 1998; *Conte et al.*, 2006]. In general, the reconstruction of modern and past sea surface temperatures using alkenones may be limited by lateral advection, especially in regions underlying strong currents and at oceanic frontal systems with large temperature and productivity gradients. A similar influence on proxy signals is likely for other recorders of oceanic properties such as planktic microfossils (e.g., foraminifera, diatoms, radiolarians) or bulk sediment constituents (organic carbon, carbonate, opal, clay minerals), depending on their respective particle size.

Acknowledgments

[25] We thank H. Andruleit, J. Knies, S. Mulitza, M. Prange, S. Schulte, and A. Vink for discussions and suggestions concerning this manuscript, U. Groß and A. de Leon for help with sampling, R. Kreutz for assistance with the gas chromatograph, and two anonymous reviewers for their constructive comments. This work was funded by the Deutsche Forschungsgemeinschaft (DFG).

References

Andruleit, H., U. Rogalla, and S. Stäger (2004), From living communities to fossil assemblages: origin and fate of coccolithophores in the northern Arabian Sea, *Micropaleontology*, *50*, 5–21.

Bac, M., K. R. Buck, F. P. Chavez, and S. C. Brassell (2003), Seasonal variation in alkenones, bulk suspended POM, plankton and temperature in Monterey Bay, California: Implications for carbon cycling and climate assessment, *Org. Geochem.*, *34*, 837–855.

Bendle, J., and A. Rosell-Melé (2004), Distributions of U^{K}_{37} and $U^{K'}_{37}$ in the surface waters and sediments of the Nordic Seas: Implications for paleoceanography, *Geochem. Geophys. Geosyst.*, *5*, Q11013, doi:10.1029/2004GC000741.

Bentaleb, I., J. O. Grimalt, F. Vidussi, J.-C. Marty, V. Martin, M. Denis, C. Hatté, and M. Fontugne (1999), The C_{37} alkenone record of seawater temperature during seasonal thermocline stratification, *Mar. Chem.*, *64*, 301–313.

Bentaleb, I., M. Fontugne, and L. Beaufort (2002), Long-chain alkenones and $U^{K'}_{37}$ variability along a south-north transect in the western Pacific Ocean, *Global Planet. Change*, *34*, 173–183.

Benthien, A., and P. J. Müller (2000), Anomalously low alkenone temperatures caused by lateral particle and sediment transport in the Malvinas Current region, western Argentine Basin, *Deep Sea Res., Part I*, *47*, 2369–2393.

Bianchi, A. A., C. F. Giulivi, and A. R. Piola (1993), Mixing in the Brazil-Malvinas Confluence, *Deep Sea Res., Part I*, *40*, 1345–1358.

Boltovskoy, D. (1994), The sedimentary record of pelagic biogeography, *Progr. Oceanogr.*, *34*, 135–160.

Boltovskoy, E., D. Boltovskoy, N. Correa, and F. Brandini (1996), Planktic foraminifera from the southwestern Atlantic (30°–60°S): Species-specific patterns in the upper 50 m, *Mar. Micropaleontol.*, *28*, 53–72.

Brandini, F. P., D. Boltovskoy, A. Piola, S. Kocmur, R. Rottgers, P. C. Abreu, and R. M. Lopes (2000), Multiannual trends in fronts and distribution of nutrients and chlorophyll in the southwestern Atlantic (30–62°S), *Deep Sea Res., Part I*, *47*, 1015–1033.

Brassell, S. C., G. Eglinton, I. T. Marlowe, U. Pflaumann, and M. Sarntheim (1986), Molecular stratigraphy: A new tool for climatic assessment, *Nature*, *320*, 129–133.

Brown, C. W., and G. P. Podestá (1997), Remote sensing of coccolithophore blooms in the western South Atlantic Ocean, *Remote Sens. Environ.*, *60*, 83–91.

Butzin, M., M. Prange, and G. Lohmann (2005), Radiocarbon simulations for the glacial ocean: The effects of wind stress, Southern Ocean sea ice and Heinrich events, *Earth Planet. Sci. Lett.*, *235*, 45–61.

Cacho, I., C. Pelejero, J. O. Grimalt, A. Calafat, and M. Canals (1999), C_{37} alkenone measurements of sea surface temperature in the Gulf of Lions (NW Mediterranean), *Org. Geochem.*, *30*, 557–566.

Carreto, J. I., V. A. Lutz, M. O. Carignan, A. D. Cucchi Colleoni, and S. G. de Marco (1995), Hydrography and chlorophyll a in a transect from the coast to the shelf-break in the Argentinian Sea, *Cont. Shelf Res.*, *15*, 315–336.

Conkright, M. E., et al. (2002), *World Ocean Database 2001,* vol. 1, *Introduction*, edited by S. Levitus. *NOAA Atlas NESDIS 42*, 167 pp., NOAA, Silver Spring, Md.

Conte, M. H., and G. Eglinton (1993), Alkenone and alkenoate distributions within the euphotic zone of the eastern North Atlantic: Correlation with production temperature, *Deep Sea Res., Part I*, *40*, 1935–1961.

Conte, M. H., A. Thompson, and G. Eglinton (1994), Primary production of lipid biomarker compounds by *Emiliania huxleyi*: Results from an experimental mesocosm study in Korsfjorden, southern Norway, *Sarsia*, *79*, 319–332.

Conte, M. H., A. Thompson, D. Lesley, and R. P. Harris (1998), Genetic and physiological influences on the alkenone/alkenoate versus growth temperature relationship in *Emiliania huxleyi* and *Gephyrocapsa oceanica*, *Geochim. Cosmochim. Acta*, *62*, 54–68.

Conte, M. H., M. Sicre, C. Rühlemann, J. C. Weber, S. Schulte, D. Schulz-Bull, and T. Blanz (2006), Global tem-

perature calibration of the alkenone unsaturation index ($U^{K'}_{37}$) in surface waters and comparison with surface sediments, *Geochem. Geophys. Geosyst.*, *7*, Q02005, doi:10.1029/2005GC001054.

Davis, J. C. (1986), *Statistics and Data Analysis in Geology*, 646 pp., John Wiley, Hoboken, N. J.

Divine, D. V., and C. Dick (2006), Historical variability of sea ice edge position in the Nordic Seas, *J. Geophys. Res.*, *111*, C01001, doi:10.1029/2004JC002851.

Eppley, R. W., E. H. Renger, and P. R. Betzer (1983), The residence time of particulate organic carbon in the surface layer of the ocean, *Deep Sea Res.*, *30*, 311–323.

Epstein, B. L., S. D'Hondt, J. G. Quinn, J. Zhang, and P. E. Hargraves (1998), An effect of dissolved nutrient concentrations on alkenone-based temperature estimates, *Paleoceanography*, *13*, 122–126.

Gayoso, A. M. (1995), Bloom of *Emiliania huxleyi* (Prymnesiophyceae) in the western South Atlantic Ocean, *J. Plankton Res.*, *17*, 1717–1722.

Goni, G., S. Kamholz, S. Garzoli, and D. Olson (1996), Dynamics of the Brazil-Malvinas Confluence based on inverted echo sounders and altimetry, *J. Geophys. Res.*, *101*, 16,273–16,289.

Hamanaka, J., K. Sawada, and E. Tanoue (2000), Production rates of C_{37} alkenones determined by ^{13}C labeling technique in the euphotic zone of Sagami Bay, Japan, *Org. Geochem.*, *31*, 1095–1102.

Harada, N. K., H. Shin, A. Murata, M. Uchida, and T. Nakatani (2003), Characteristics of alkenones synthesized by a bloom of *Emiliania huxleyi* in the Bering Sea, *Geochim. Cosmochim. Acta*, *67*, 1507–1519.

Hentschel, E. (1936), Allgemeine Biologie des südatlantischen Ozeans, *Wiss. Ergeb. Dtsch. Atl. Exped.*, *11*, 344 pp.

Jones, G. A., and D. A. Johnson (1984), Displaced Antarctic diatoms in Vema Channel sediments: Late Pleistocene/Holocene fluctuations in AABW flow, *Mar. Geol.*, *58*, 165–186.

Jordan, R. W., and A. Kleijne (1994), A classification system for living coccolithophores, in *Coccolithophores*, edited by A. Winter and W. G. Siesser, pp. 83–106, Cambridge Univ. Press, New York.

Maier-Reimer, E., U. Mikolajewicz, and K. Hasselmann (1993), Mean circulation of the Hamburg LSG OGCM and its sensitivity to the thermohaline surface forcing, *J. Phys. Oceanogr.*, *23*, 731–757.

McCave, I. N. (1975), Vertical flux of particles in the ocean, *Deep Sea Res.*, *22*, 491–502.

Moran, S. B., and J. N. Smith (2000), ^{234}Th as a tracer of scavenging and particle export in the Beaufort Sea, *Cont. Shelf Res.*, *20*(2), 153–167.

Mollenhauer, G., J. F. McManus, A. Benthien, P. J. Müller, and T. I. Eglinton (2006), Rapid lateral particle transport in the Argentine Basin: Molecular ^{14}C and $^{230}Th_{xs}$ evidence, *Deep Sea Res., Part I*, *53*, 1224–1243.

Müller, P. J., and G. Fischer (2004), C_{37} alkenones as paleotemperature tool: Fundamentals based on sediment traps and surface sediments from the South Atlantic Ocean, in *The South Atlantic in the Late Quaternary: Reconstruction of Material Budget and Current Systems*, edited by G. Wefer, S. Mulitza, and V. Ratmeyer, pp. 169–195, Springer, New York.

Müller, P. J., G. Kirst, G. Ruhland, I. von Storch, and A. Rosell-Melé (1998), Calibration of the alkenone paleotemperature index $UK'37$ based on core-tops from the eastern South Atlantic and the global ocean (60°N–60°S), *Geochim. Cosmochim. Acta*, *62*, 1757–1772.

Ohkouchi, N., T. L. Eglinton, L. D. Keigwin, and J. M. Hayes (2002), Spatial and temporal offsets between proxy records in a sediment drift, *Science*, *298*, 1224–1227.

Okada, H., and S. Honjo (1975), Distribution of coccolithophores in marginal seas along the western Pacific Ocean and in the Red Sea, *Mar. Biol.*, *31*, 271–285.

Olson, D. B., G. P. Podestá, R. H. Evans, and O. B. Brown (1988), Temporal variations in the separation of Brazil and Malvinas Currents, *Deep Sea Res.*, *35*, 1971–1990.

Peterson, R. G., and L. Stramma (1991), Upper-level circulation in the South Atlantic Ocean, *Progr. Oceanogr.*, *26*, 1–73.

Peterson, R. G., C. S. Johnson, W. Krauss, and R. E. Davis (1996), Lagrangian measurements in the Malvinas Current, in *The South Atlantic: Present and Past Circulation*, edited by G. Wefer et al., pp. 239–247, Springer, New York.

Piola, A. R., and R. P. Matano (2001), Brazil and Falklands (Malvinas) Currents, in *Encyclopedia of Ocean Sciences*, edited by J. H. Steele, pp. 340–349, Elsevier, New York.

Popp, B. D., F. Kenig, S. G. Wakeham, E. A. Laws, and R. R. Bidigare (1998), Does growth rate affect ketone unsaturation and intracellular carbon isotopic variability in *Emiliania huxleyi*?, *Paleoceanography*, *13*, 35–41.

Prahl, F. G., and S. G. Wakeham (1987), Calibration of unsaturation patterns in long-chain ketone compositions for palaeotemperature assessment, *Nature*, *330*, 367–369.

Prahl, F. G., L. A. Muehhausen, and D. L. Zahnle (1988), Further evaluation of long-chain alkenones as indicators of paleoceanographic conditions, *Geochim. Cosmochim. Acta*, *52*, 2303–2310.

Prahl, F. G., G. L. Cowie, G. J. D. Lange, and M. A. Sparrow (2003), Selective organic matter preservation in "burn-down" turbidites on the Madeira Abyssal Plain, *Paleoceanography*, *18*(2), 1052, doi:10.1029/2002PA000853.

Prahl, F. G., B. N. Popp, D. M. Karl, and M. A. Sparrow (2005), Ecology and biogeochemistry of alkenone production at Station ALOHA, *Deep Sea Res., Part I*, *52*, 699–719.

Prange, M., G. Lohmann, and A. Paul (2003), Influence of vertical mixing on the thermohaline hysteresis: Analyses of an OGCM, *J. Phys. Oceanogr.*, *33*, 1707–1721.

Provost, C., S. Gana, V. Garcon, K. Maamaatuaiahutapu, and M. England (1995), Hydrographic conditions in the Brazil-Malvinas confluence during austral summer 1990, *J. Geophys. Res.*, *100*, 10,655–10,678.

Provost, C., V. Garçon, and L. M. Falcon (1996), Hydrographic conditions in the surface layers over the slope-open ocean transition area near the Brazil-Malvinas Confluence during austral summer 1990, *Cont. Shelf Res.*, *16*, 215–235.

Riebesell, U., A. T. Revill, D. G. Holdsworth, and J. K. Volkman (2000), The effects of varying CO_2 concentration on lipid composition and carbon isotope fractionation in *Emiliania huxleyi*, *Geochim. Cosmochim. Acta*, *64*, 4179–4192.

Rosell-Melé, A., G. Eglinton, U. Pflaumann, and M. Sarnthein (1995), Atlantic core-top calibration of the $UK'37$ index as a sea-surface paleotemperature indicator, *Geochim. Cosmochim. Acta*, *59*, 3099–3107.

Sachs, J. P., and R. F. Anderson (2003), Fidelity of alkenone paleotemperatures in southern Cape Basin sediment drifts, *Paleoceanography*, *18*(4), 1082, doi:10.1029/2002PA000862.

Sawada, K., N. Handa, Y. Shiraiwa, A. Danbara, and S. Montani (1996), Long-chain alkenones and alkyl alkenoates in the coastal and pelagic sediments of the northwest North Pacific, with special reference to the reconstruction

of *Emiliania huxleyi* and *Gephyrocapsa oceanica* ratios, *Org. Geochem.*, *24*, 751–764.

Sawada, K., N. Handa, and T. Nakatsuda (1998), Production and transport of long-chain alkenone and alkyl alkenoates in a sea water column in the northwestern Pacific off central Japan, *Mar. Chem.*, *59*, 219–234.

Schäfer-Neth, C., and A. Paul (2001), Circulation of the glacial Atlantic: A synthesis of global and regional modeling, in *The Northern North Atlantic: A Changing Environment*, edited by P. Schäfer et al., pp. 446–462, Springer, New York.

Schmidt, S., V. Andersen, S. Belviso, and J.-C. Marty (2002a), Strong seasonality in particle dynamics of north-western Mediterranean surface waters as revealed by $^{234}Th/^{238}U$, *Deep Sea Res., Part I*, *49*, 1507–1518.

Schmidt, S., L. Chou, and I. A. Hall (2002b), Particle residence times in surface waters over the north-western Iberian Margin: Comparison of pre-upwelling and winter periods, *J. Mar. Syst.*, *32*, 3–11.

Shin, K.-H., N. Tanaka, N. Harada, and J.-C. Marty (2002), Production and turnover rates of C_{37} alkenones in the eastern Bering Sea: Implication for the mechanism of a long duration of *Emiliani huxleyi* bloom, *Prog. Oceanogr.*, *55*, 113–129.

Sicre, M.-A., Y. Ternois, J.-C. Miquel, and J.-C. Marty (1999), Alkenones in the northwestern Mediterranean Sea: Interannual variability and vertical transfer, *Geophys. Res. Lett.*, *26*, 1735–1738.

Sicre, M. A., L. Labeyrie, U. Ezat, J. Duprat, J. L. Turon, S. Schmidt, E. Michel, and A. Mazaud (2005), Mid-latitude southern Indian Ocean response to Northern Hemisphere Heinrich events, *Earth Planet. Sci. Lett.*, *240*, 724–731.

Sikes, E. L., and M.-A. Sicre (2002), Relationship of the tetra-unsaturated C_{37} alkenone to salinity and temperature: Implications for paleoproxy applications, *Geochem. Geophys. Geosyst.*, *3*(11), 1063, doi:10.1029/2002GC000345.

Sikes, E. L., and J. K. Volkman (1993), Calibration of alkenone unsaturation ratios ($UK'37$) for paleotemperature estimation in cold polar waters, *Geochim. Cosmochim. Acta*, *57*, 1883–1889.

Sikes, E. L., J. W. Farrington, and L. D. Keigwin (1991), Use of the alkenone unsaturation ratio Uk37 to determine past sea surface temperatures: Core-top SST calibrations and methodology considerations, *Earth Planet. Sci. Lett.*, *104*, 36–47.

Sikes, E. L., J. K. Volkman, L. G. Robertson, and J.-J. Pichon (1997), Alkenones and alkenes in surface waters and sediments of the Southern Ocean: Implications for paleotemperature estimation in polar regions, *Geochim. Cosmochim. Acta*, *61*, 1495–1505.

Ternois, Y., M.-A. Sicre, A. Boireau, M. H. Conte, and G. Eglinton (1997), Evaluation of long-chain alkenones as paleo-temperature indicators in the Mediterranean Sea, *Deep Sea Res., Part I*, *44*, 271–286.

Thomsen, C., D. E. Schulz-Bull, G. Petrick, and J. C. Duinker (1998), Seasonal variability of the longchain alkenone flux and the effect on the $UK'37$ index in the Norwegian Sea, *Org. Geochem.*, *28*, 311–323.

Vigan, X., C. Provost, and G. Podesta (2000), Sea surface velocities from sea surface temperature image sequences: 2. Application to the Brazil-Malvinas Confluence area, *J. Geophys. Res.*, *105*, 19,515–19,534.

Vivier, F., and C. Provost (1999), Direct velocity measurements in the Malvinas Current, *J. Geophys. Res.*, *104*, 21,083–21,103.

Volkman, J. K., and E. Tanoue (2002), Chemical and biological studies of particulate organic matter in the ocean, *J. Oceanogr.*, *58*, 265–279.

Volkman, J. K., S. M. Barrett, S. I. Blackburn, and E. L. Sikes (1995), Alkenones in *Gephyrocapsa oceanica*: Implications for studies of paleoclimate, *Geochim. Cosmochim. Acta*, *59*, 513–520.

Winter, A., R. W. Jordan, and P. H. Roth (1994), Biogeography of living coccolithophores in ocean waters, in *Coccolithophores*, edited by A. Winter and W. G. Siesser, pp. 161–178, Cambridge Univ. Press, New York.

Young, J. R., and P. R. Bown (1997), Cenozoic calcareous nannoplankton classification, *J. Nannoplankton Res.*, *19*, 36–47.